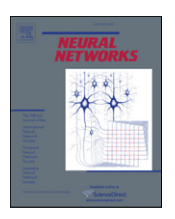
ELSEVIER

Contents lists available at ScienceDirect

#### Neural Networks

journal homepage: www.elsevier.com/locate/neunet



2008 Special Issue

## Power quality control of an autonomous wind-diesel power system based on hybrid intelligent controller

Hee-Sang Ko<sup>a</sup>, Kwang Y. Lee<sup>b</sup>, Min-Jae Kang<sup>c</sup>, Ho-Chan Kim<sup>c,\*</sup>

- <sup>a</sup> Product Development Team/Wind Turbine Division, Samsung Heavy Industries Company, Republic of Korea
- <sup>b</sup> Department of Electrical and Computer Engineering, Baylor University, USA
- <sup>c</sup> Faculty of Electrical and Electronics Engineering, Cheju National University, Republic of Korea

#### ARTICLE INFO

# Article history: Received 1 May 2008 Received in revised form 9 October 2008 Accepted 14 October 2008

Keywords:
Wind power generation
Fuzzy controller
Neural network inverse model

#### ABSTRACT

Wind power generation is gaining popularity as the power industry in the world is moving toward more liberalized trade of energy along with public concerns of more environmentally friendly mode of electricity generation. The weakness of wind power generation is its dependence on nature—the power output varies in quite a wide range due to the change of wind speed, which is difficult to model and predict. The excess fluctuation of power output and voltages can influence negatively the quality of electricity in the distribution system connected to the wind power generation plant. In this paper, the authors propose an intelligent adaptive system to control the output of a wind power generation plant to maintain the quality of electricity in the distribution system. The target wind generator is a cost-effective induction generator, while the plant is equipped with a small capacity energy storage based on conventional batteries, heater load for co-generation and braking, and a voltage smoothing device such as a static Var compensator (SVC). Fuzzy logic controller provides a flexible controller covering a wide range of energy/voltage compensation. A neural network inverse model is designed to provide compensating control amount for a system. The system can be optimized to cope with the fluctuating market-based electricity price conditions to lower the cost of electricity consumption or to maximize the power sales opportunities from the wind generation plant.

© 2008 Elsevier Ltd. All rights reserved.

#### 1. Introduction

In remote areas such as small islands, diesel generators are the main power supply. Diesel fuel has several drawbacks: it is expensive because transportation to remote areas adds extra cost, and it causes air pollution by engine exhaust. Providing a feasible economical and environmental solution to diesel generators is important. A hybrid system of wind power and diesel generators can benefit islands or other isolated communities and increase fuel savings. Wind is, however, a natural energy source that produces a fluctuating power output. The excessive fluctuations of power output adversely affect the quality of power in the distribution system, particularly frequency and voltage (Feris, 1990; Hunter & Elliot, 1994). Autonomous renewable energy systems such as wind, solar, and micro-hydro require control methods to maintain stability due to the real-time variation of input energy and load, while maximizing the use of the renewable resources.

Since the early eighties, the wind-diesel autonomous power system (WDAPS) has been accepted and widely used as electricity

generating systems for remote areas. In such cases, the WDAPS serves an entire isolated load and is responsible for maintaining frequency and voltage stability. The main driving force in WDAPS design was to secure both fuel saving and reliable power supply. Usually, diesel generator installed capacity is sized to meet the peak power demand, but is used in practice to supply power only when the wind power output is insufficient to meet the load demand (Karaki, Chedid, & Ramadan, 2000).

The random power disturbances at the output of wind-turbine generators can cause relatively large frequency and voltage fluctuations. In a large power system network, these fluctuations can have little effect on the overall quality of the delivered energy. However, with weak autonomous networks, these power fluctuations can have a marked effect, which must be eliminated regardless of the penetration rate, that is to say, the rate of wind power with respect to the power from a conventional power plant in the power system network (Chedid, Karaki, & Chadi, 2000; Pandiaraj, Taylor, & Jenkins, 2001). Hence, the control of the voltage and frequency of a weak-wind-diesel system is considered more challenging than that in large grids.

The hybrid strategy is motivated with the hope that an effective combination of controllers might improve the control performance. Since the PID controller is simple to understand

<sup>\*</sup> Corresponding author. Tel.: +82 64 754 3676; fax: +82 64 756 5281. E-mail address: hckim@cheju.ac.kr (H.-C. Kim).

and tune, it is dominantly used in industrial systems (Hagan & Menhaj, 1994). However, it is difficult to obtain good performance from the PID controller only because a nonlinearity makes control with a PID controller difficult unless gain scheduling is used. Linearizable systems can be controlled by conventional linear controllers such as state space method, optimal control, robust control, model predictive control, etc. Neural network, fuzzy logic and genetic algorithm are widely studied to deal with highly nonlinear systems.

The feedforward control concept has attractive features of practical relevance. Since it is assumed that a stabilizing controller is available in advance, the experiment to collect a set of training data sets is easily performed. Another feature is that one can introduce the feedforward signal gradually. In applications where an inappropriate control input can cause damage, this can be a soft control strategy (Madsen, 1995).

The main reasons for using feedback are to stabilize unstable systems and to reduce the influence from possible disturbances and model inaccuracies. Using feedback to ensure that the system rapidly follows changes in the reference is not always a good practice. A rapid reference tracking obtained with feedback generally has the side effect that the controller becomes highly sensitive to noise which implies the poor robust properties. To achieve a satisfying reference tracking without feedback, the feedforward is applied which is governed only by the reference. Moreover, feedforward control is used for regulation where the reference attains constant levels for longer periods of time. To speed up the tracking of set-point changes, a feedforward controller is typically designed to provide the steady-state value of the control signal for minimizing tracking error (Haley, Soloway, & Gold, 1999; Madsen, 1995).

In this paper, fuzzy-neural hybrid controller is proposed and applied for pitch control of wind turbine. Fuzzy logic is applied for designing a feedback controller. Neural network inverse model is designed for a dynamic feedforward controller. Therefore, fast damping from fuzzy controller and fast reference tracking can be accomplished.

#### 2. System description

The wind-diesel autonomous power system consists of the wind turbine having the induction generator (IG), the diesel engine (DE), synchronous generator (SG), superconducting magnetic energy storage (SMES), and the dumpload. When wind generated power is sufficient to serve the load, the DE is disconnected from the SG by electromagnetic clutch, and the synchronous generator acts as a synchronous condenser. The main purpose of the dumpload is to regulate the system frequency. The SG (with/without diesel) is used for reactive power control that is achieved by the excitation system to regulate voltage. The SG also contributes the reactive power to compensate the induction generator.

SMES is a control unit for a synchronous machine (Tripathy, Kalantar, & Balasubramanian, 1991). When there is a sudden rise in the demand of load, the stored energy is immediately released through the power system. As the governor and pitch control mechanism start working to set the power system to the new operating condition, a SMES unit charges back to its initial value of current. In the case of sudden release of the loads, a SMES immediately gets charged towards its full value, thus absorbing some portion of the excess energy in the system, and as the system returns to its steady state, the excess energy absorbed is released and SMES current attains its normal value.

Fig. 1 shows the prototype of a wind–diesel autonomous power system (Chedid et al., 2000). Generator dynamics model consists of a synchronous machine driven by diesel engine through flywheel and connected in parallel with an induction machine driven by a wind turbine.

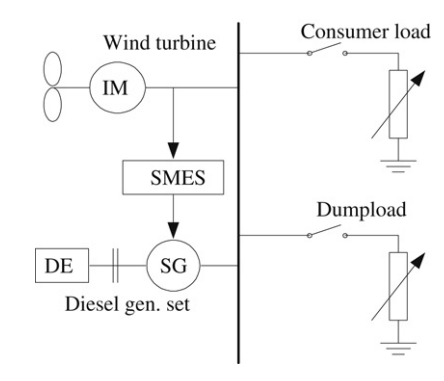


Fig. 1. The prototype of wind-diesel autonomous power system.

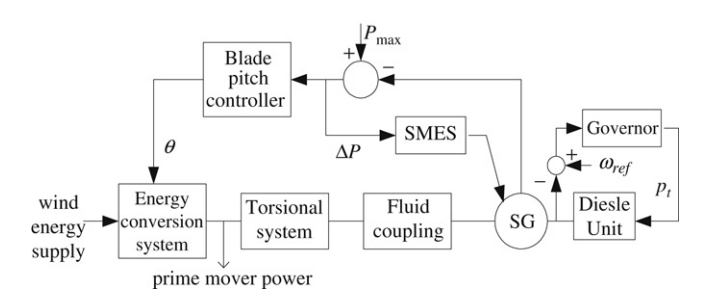


Fig. 2. The basic configuration of WDAPS.

Blade pitch control of wind turbine has the potential for producing the highest level of interaction because of the presence of both diesel and wind-turbine control loops (Tripathy et al., 1991). The pitch control system consists of a power measurement transducer, a manual power set-point control, a proportional plus integral feedback function, and hydraulic actuator, which varies the pitch of the blades. Turbine blade pitch control has a significant impact on the dynamic behavior of the system. Variable pitch turbines operate efficiently over a wider range of wind speeds than fixed pitch machines. The generator dynamics model consists of a synchronous generator driven by a diesel engine through a flywheel and connected in parallel with an induction generator driven by a wind turbine. The diesel generator will act as a dummy grid for the wind generator, which is connected in parallel. When wind power rises above the power set point and SMES unit is fully charged, the pitch control system begins to operate to maintain an average power equal to the set point. The study in this paper is focused on the designing of turbine blade pitch controller based on fuzzy logic and neural network.

The simplified description of Fig. 1 is in Fig. 2 with SMES (Tripathy et al., 1991).

The models of the generators are based on the standard Park's transformation (Krause, Wasynczuk, & Sudhoff, 1986) that transforms all stator variables to a rotor reference frame described by a direct and quadrature (d-q) axis. The set of SG and IG equations are based on the d-q-axis in accordance with (International Electrotechnical Commission, 1975). The SMES model can be found in Tripathy et al. (1991).

The nonlinear mathematical model of the wind-diesel power system is given in detail in Appendix A. The following considerations are taken into account to identify component models: the electrical system is assumed as a perfectly balanced three-phase system with pure sinusoidal voltage and frequency. High frequency transients in stator variables are neglected, which indicates that the stator voltage and currents are allowed to change instantly. This is because this paper is focused on the transient period instead of sub-transient period. Damper-winding models are ignored because their effect appears mainly in a grid-connected

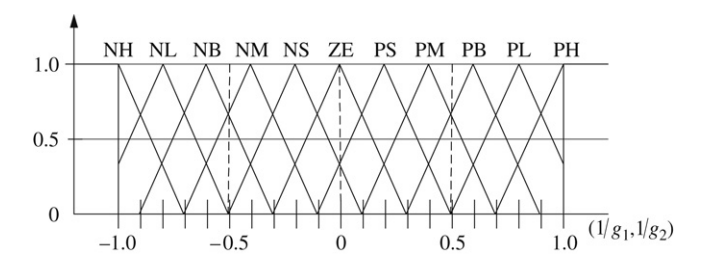


Fig. 3. Membership function of error and change in error.

system or a system with several synchronous generators running in parallel. The different component models are of equal level of complexity.

#### 3. Fuzzy-neural hybrid control

#### 3.1. Feedback controller based on fuzzy logic

Fuzzy control systems are rule-based systems in which a set of fuzzy rules represents a control decision mechanism to adjust the effects of certain system conditions. Fuzzy controller is based on the linguistic relationships or rules that define the control laws of a process between input and output (Passino, 1997; Yen & Langari, 1999). This feature draws attention toward a fuzzy controller due to its nonlinear characteristics and no need for an accurate system modeling. The fuzzy controller consists of rule base, which represents a fuzzy logic quantification of the expert's linguistic description of how to achieve good control, fuzzification of actual input values, fuzzy inference, and defuzzification of fuzzy output. When the expert's linguistic description is not available, fuzzy controller still can be designed by using the measurement of real-time input/output data (Park, Moon, & Lee, 1995, 1996)

In this paper, a total of 121 rules are used for the power system under study. The general form of the fuzzy rule is given in the *if-then* form as follows:

if 
$$x(k)$$
 is A and  $\Delta x(k)$  is B, then  $y(k)$  is C, (1)

where

x,  $\Delta x$ : input signals,

y: controller output,

A, B, C: linguistic variables.

The linguistic values extracted from the experimental knowledge are NH (negative high), NL (negative large), NB (negative big), NM (negative medium), NS (negative small), ZE (zero), PS (positive small), PM (positive medium), PB (positive big), PL (positive large), and PH (positive high).

In the power system under study, generator power deviation  $(\Delta P)$  is chosen for the input of a fuzzy controller. The linguistic descriptions provide experimental expressions of the expert for a control decision-making process and each linguistic variable is represented as triangular membership functions shown in Figs. 3 and 4. In the fuzzy controller, the input normalization factors are chosen to represent the proper membership quantifications of linguistic values. In addition, normalization factors can be used to yield the desired response of the fuzzy controller,  $g_1$ ,  $g_2$  stand for a normalization factor for input of fuzzy controller and  $g_0$  stands for a denormalization factor for output of fuzzy controller. Fig. 3 shows the membership function for error and change in error and Fig. 4 depicts the membership function for output.

In Figs. 3 and 4, the membership functions are overlapped with each other to smooth a fuzzy system output and a fuzzy controller is designed to regulate a system smoothly when an error and a change in error are near zero. The rules are established to control transient stability problem for all possible cases. Tables 1 and 2 show the inference rule table for two input fuzzy variables in negative and positive sides of change in error, respectively.

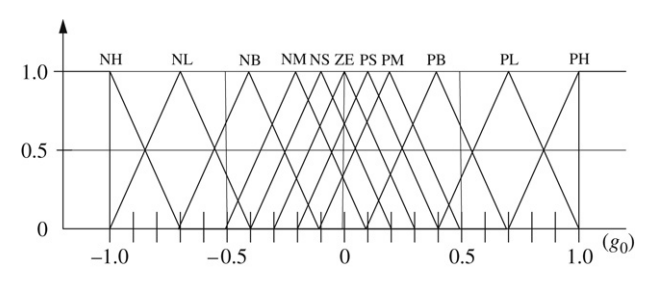


Fig. 4. Membership function of output.

**Table 1**Inference rule table in negative side of change in error.

Error		Change in error						
		-1	-0.8	-0.6	-0.4	-0.2	0	
	-1	-1	-1	-1	-1	-1	-1	
	-0.8	-1	-1	-1	-1	-1	-0.7	
	-0.6	-1	-1	-1	-1	-0.7	-0.4	
	-0.4	-1	-1	-1	-0.7	-0.4	-0.2	
	-0.2	-1	-1	-0.7	-0.4	-0.2	-0.1	
	0	-1	-0.7	-0.4	-0.2	-0.1	0	
	0.2	-0.7	-0.4	-0.2	-0.1	0	0.1	
	0.4	-0.4	-0.2	-0.1	0	0.1	0.2	
	0.6	-0.2	-0.1	0	0.1	0.2	0.4	
	0.8	-0.1	0	0.1	0.2	0.4	0.7	
	1	0	0.1	0.2	0.4	0.7	1	

**Table 2** Inference rule table in positive side of change in error.

0.2 -1	0.4 -1	0.6 -1	0.8	1
-	-1	1		
		-1	-1	-1
-0.4	-0.2	-0.1	0	-0.7
-0.2	-0.1	0	0.1	-0.4
-0.1	0	0.1	0.2	-0.2
0	0.1	0.2	0.4	-0.1
0.1	0.2	0.4	0.7	0
0.2	0.4	0.7	1	0.1
0.4	0.7	1	1	0.2
0.7	1	1	1	0.4
1	1	1	1	0.7
1	1	1	1	1
	-0.1 0 0.1 0.2 0.4	$\begin{array}{ccc} -0.2 & -0.1 \\ -0.1 & 0 \\ 0 & 0.1 \\ 0.1 & 0.2 \\ 0.2 & 0.4 \\ 0.4 & 0.7 \end{array}$	$\begin{array}{ccccc} -0.2 & -0.1 & 0 \\ -0.1 & 0 & 0.1 \\ 0 & 0.1 & 0.2 \\ 0.1 & 0.2 & 0.4 \\ 0.2 & 0.4 & 0.7 \\ 0.4 & 0.7 & 1 \\ \end{array}$	$\begin{array}{cccccccccccccccccccccccccccccccccccc$

It is required to find the fuzzy region for the output for each rule. The centroid or the center of gravity defuzzification method (Yen & Langari, 1999) is used which calculates the most typical crisp value of the fuzzy set and "y is C" in Eq. (1) can be expressed by (2).

$$y = \frac{\sum_{i} \mu_{A}(y_{i}) \times y_{i}}{\sum_{i} \mu_{A}(y_{i})}$$
 (2)

where  $\mu_A$  is a degree of the membership function.

### 3.2. Feedforward compensator based on neural network inverse model

A neural network can model an input/output relationship of a dynamic system. A direct or forward model is a mapping that maps a system input to a system output. An inverse model, on the other hand, is an inverse mapping that maps a system output to a system input. In particular, if one sets the output to be the reference, then the inverse model could give a desired input for the output to follow the reference or set point. The concept of inverse model was used in designing feedforward controls for dynamic systems (Harnold, Lee, Lee, & Park, 1998; Kawato, Furukawa, & Suzuki, 1987; Nakanishi & Schaal, 2004; Park, Choi, & Lee, 1996). Kawato et al. (1987) applied the concept of inverse-dynamics

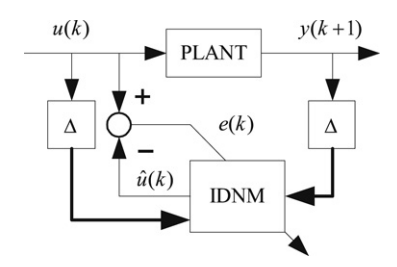


Fig. 5. Training mode of NNIM.

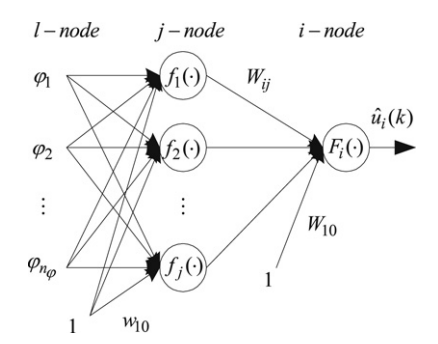


Fig. 6. Neural Network Inverse Model (NNIM).

model to control a three-joint robotic manipulator represented in a continuous nonlinear kinematics model. In view of the fact that the inverse-dynamics model only gives the ideal computed torque, feedback-error-learning scheme was utilized to compensate for the output error. Nakanishi and Schaal (2004) reformulated the feedback-learning scheme for a class of nonlinear systems from a viewpoint of the nonlinear adaptive control theory. Park and Choi et al. (1996) and Harnold et al. (1998) approached the problem from the viewpoint of discrete-time model of the nonlinear system, thus avoiding the issues of the invertibility of a nonlinear model.

A two layer neural network is applied to obtain a dynamic feedforward compensator (Haykin, 1998). In general, the output of a system can be described with a function or a mapping of the plant input–output history (Haykin, 1998; Ng, 1997). For a single-input single-output (SISO) discrete-time system, the mapping can be written in the form of a nonlinear function as follows:

$$y(k+1) = f(y(k), y(k-1), \dots, y(k-n), u(k), u(k-1), \dots, u(k-m)).$$
(3)

Solving for the control, (3) can be represented as the following:

$$u(k) = g(y(k+1), y(k), y(k-1), y(k-2), \dots, y(k-n), u(k-1), u(k-2), u(k-3), \dots, u(k-m)),$$
(4)

which is a nonlinear inverse mapping of (3). The objective of the control problem is to find a control sequence, which will drive a system to an arbitrary reference trajectory. This can be achieved by replacing y(k+1) in (4) with reference output  $y_{ref}$  or the temporary target  $y_r(k+1)$ , evaluated by

$$y_r(k+1) = y(k) + \alpha(y_{ref} - y(k)),$$
 (5)

where  $\alpha$  is the target ratio constant  $(0 < \alpha \le 1)$ . The value of  $\alpha$  describes the rate with which the present output y(k) approaches the reference output value, and thus has a positive value between 0 and 1 (Park et al., 1995; Park & Moon et al., 1996). In Fig. 5, the training mode is introduced, where  $\Delta$  denotes the vector of delay sequence data. Fig. 6 shows the neural network inverse model (NNIM) in training mode. All activation functions in the hidden layer are  $\tanh(x)$  (described as  $f_j$  in Fig. 6) and the activation function in output layer is x (depicted as  $F_i$  in Fig. 6).

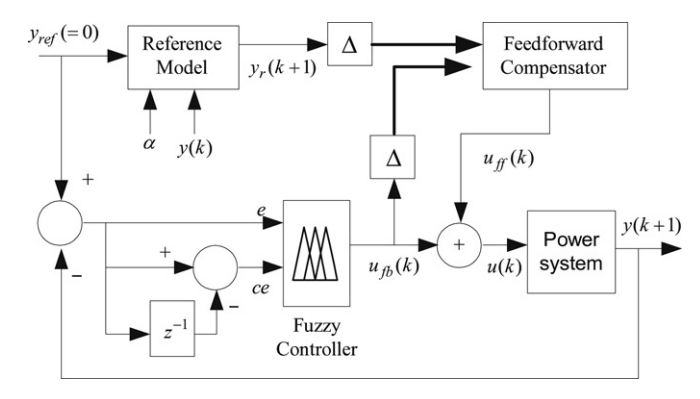


Fig. 7. The fuzzy-neural hybrid control.

The output of the NNIM can be represented as

$$\hat{u}_{i}(k) = F_{i} \left[ \sum_{j=1}^{n_{h}} W_{ij} f_{j} \left( \sum_{l=1}^{n_{\varphi}} w_{jl} \bar{\varphi} + w_{j0} \right) + W_{i0} \right], \tag{6}$$

where

$$\bar{\varphi} = [y(k+1), y(k), \dots, y(k-n), u(k-1), \dots, u(k-m)]^{T}$$
  
and  $\bar{\varphi} = [\varphi_1, \varphi_2, \varphi_3, \dots, \varphi_{n_{\omega}}]^{T}$ 

 $w_{il}$ : weight between input and hidden layers,

 $n_h$ ,  $n_{\omega}$ : number of hidden neurons and external input,

 $W_{ii}$ : weight between hidden and output layers.

The above neural network inverse model is trained based on the input–output data described in Fig. 5. To train the neural network inverse model, the Levenberg–Marquardt method is applied which is fast and robust (Haykin, 1998; Madsen, 1995; Ng, 1997). The trained NNIM is used as a feedforward compensator.

The total control scheme is indicated in Fig. 7. In the fuzzy controller, the input normalization factors are chosen to represent the proper membership quantifications of linguistic values. In addition, normalization factors can be used to yield the desired response of the fuzzy controller. The symbol  $\Delta$  denotes the vector of delay sequence data. The total control input is  $u(k) = u_{fb}(k) + u_{ff}(k)$ . The feedback control  $u_{fb}(k)$  is the output of the fuzzy controller and the output of the feedforward controller,  $u_{ff}(k)$ , can be represented as the following:

$$u_{ff}(k) = g(y_r(k+1), y_r(k), y_r(k-1), \dots, y_r(k-n), u_{fb}(k-1), u_{fb}(k-2), \dots, u_{fb}(k-m)).$$
 (7)

In Fig. 7, once a signal of a feedforward compensator is given to the control system, the fuzzy controller provides a signal that minimizes the error between the system output and its set point. This control scheme can be a soft way of generating a control signal to minimize the tracking error and improve system performance in the sense that the compensating signal is given in advance (Madsen, 1995). This implies the improvement of the existing PID-type controller, which is the main purpose of a feedforward controller in a hybrid control scheme.

#### 4. Simulation

First, a fuzzy controller is designed for a feedback controller and a neural network inverse model is obtained for a feedforward compensator. In this paper,  $\alpha$  is 0.1 and  $g_1,g_2,g_0$  are 5, 50, and 5, respectively, determined by trial and error. The Levenberg–Marquardt method is applied to train a neural network inverse model. The sampling time is 0.01 s. for the proposed control action. The training is carried out by giving varying white noise signals. Firstly, before training, fuzzy control is implemented with the plant. Secondly, white noise signal is inserted into the fuzzy controller and data set is obtained, using noise signal as input and plant output as output. Then, the neural network inverse model

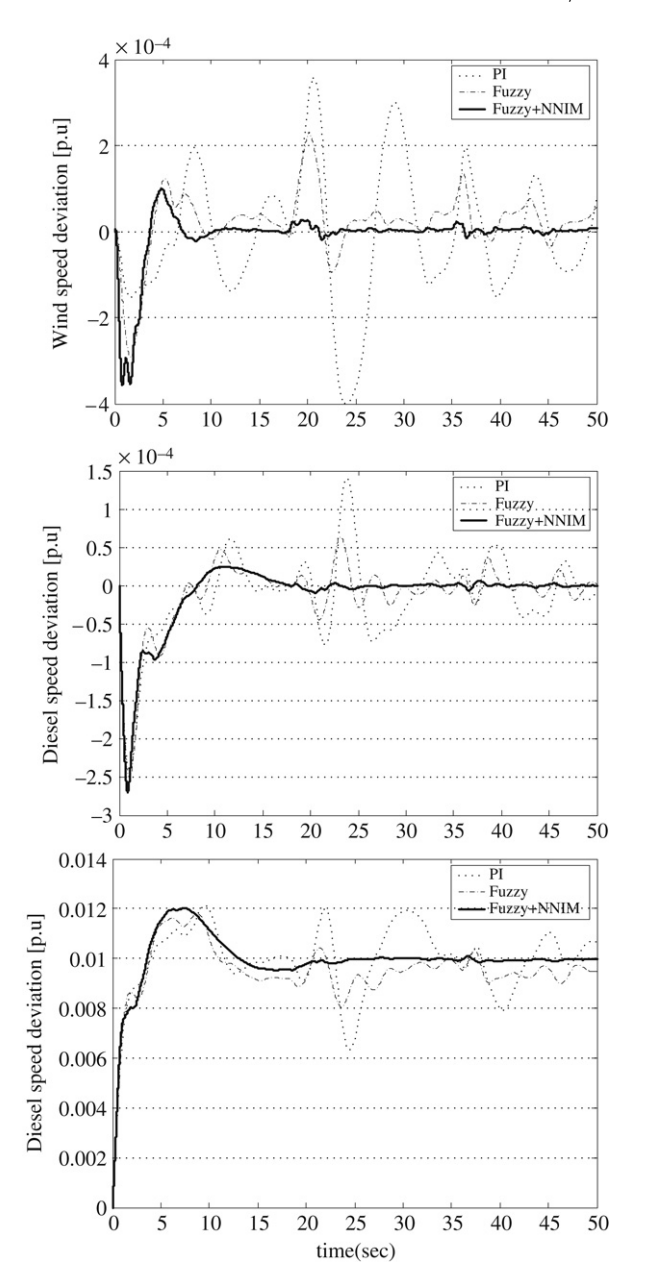


Fig. 8. Comparison of system response among PI, FC, and FNHC.

(NNIM) is trained by setting the noise signal as output and the plant output as input of the NNIM.

The proposed fuzzy-neural hybrid controller is tested in a wind-diesel autonomous power system (WDAPS). Two cases are considered: first, the sudden step load increase of 0.01 per-unit (p.u.) when SMES is in discharging mode (rectifier mode); second, when the SMES is fully discharged and there is a sudden step load increase. In this case, SMES is in recharging mode (inverter mode). (The "(p.u.)" stands for "per-unit". It is a normalized value with respect to a base or reference value.)

#### 4.1. Case 1: A sudden step load increase

The load is suddenly increased by 0.01 p.u. The SMES releases the charged current (2 p.u.). The governor and pitch mechanism start operating for charging current of SMES and damping of WDAPS. Fig. 8 shows improvement of the system frequency oscillations and power deviations, where PI stands for conventional proportional–integral controller and FC stands for fuzzy logic feedback controller.

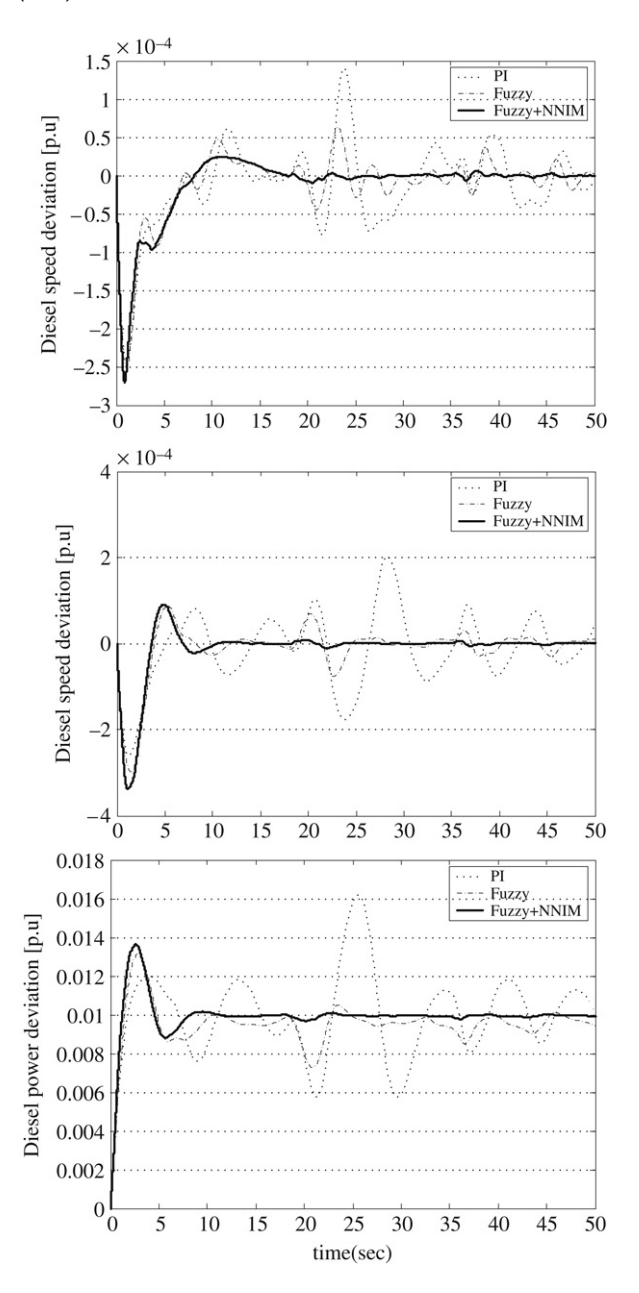


Fig. 9. Comparison of system response among PI, FC, and FNHC.

#### 4.2. Case 2: Sudden step load increase with fully discharged SMES

In this case, the SMES is fully discharged (0 p.u.). Then, the SMES needs to recharge current to the set point (2 p.u.). The wind power generation from the wind turbine is assumed to be not sufficient. Fig. 9 also shows that the FNHC performance is much better than the PI and the FC.

#### 5. Conclusion

In this paper, the fuzzy-neural hybrid controller for electricity quality control of wind power generation plants is presented. The main idea of hybrid control is that the dynamic feedforward control can be used for improving the reference tracking while feedback is used for stabilizing the system and for suppressing disturbances. Feedforward controller is a neural network inverse model (NNIM), which is trained by the Levenberg-Marquardt method, and feedback controller is a fuzzy controller.

The Fuzzy-NNIM was tested in a wind-diesel autonomous power system and compared with the conventional PI and the fuzzy controller. In all cases, the Fuzzy-NNIM out-performed the conventional PI and the fuzzy controller. The Fuzzy-NNIM provides quite small frequency deviation. Thus, the usefulness of Fuzzy-NNIM-based controller design is demonstrated.

#### Appendix A. Wind-diesel power system model (International Electrotechnical Commission, 1975; Krause et al., 1986)

A.1. Diesel-engine-Synchronous-generator model (salient pole)

$$\dot{Q}_{f} = \frac{1}{\tau_{c}} \left( -Q_{f} + Q_{d}(t - \tau_{d}) \right) 
\dot{\theta}_{cl} = \omega_{d} - \omega_{s} 
\dot{\omega}_{d} = \frac{1}{J_{d}} \left( k_{c} k_{v} Q_{f} - (D_{d} + D_{cl}) \omega_{d} + D_{cl} \omega_{s} - k_{v} p_{o} - C_{cl} \theta_{cl} \right) 
\dot{\psi}_{f} = \frac{1}{\tau'_{do}} \left( -\psi_{f} + L_{md} I_{sd} \right) + E_{fd} 
\dot{\omega}_{s} = \frac{1}{J_{s}} \left( C_{cl} \theta_{cl} + D_{cl} \omega_{d} - T_{s} - (D_{cl} + D_{s}) \omega_{s} \right) 
\begin{bmatrix} R_{s} & -\omega_{s} L'_{d} & 1 & 0 \\ \omega_{s} L_{q} & R_{s} & 0 & 1 \\ R_{1} & -\omega_{s} L_{1} & -1 & 0 \\ \omega_{s} L_{1} & R_{1} & 0 & -1 \end{bmatrix} \begin{bmatrix} I_{sq} \\ I_{sd} \\ V_{sq} \\ V_{sd} \end{bmatrix} + \begin{bmatrix} 0 & 0 \\ 0 & 0 \\ 1 & 0 \\ 0 & 1 \end{bmatrix} \begin{bmatrix} V_{bq} \\ V_{bd} \end{bmatrix} 
= \begin{bmatrix} \omega_{s} \frac{L_{md}}{L_{f}} \psi_{f} \\ 0 \\ 0 \\ 0 \end{bmatrix}$$

$$= \begin{bmatrix} \omega_{s} \frac{L_{md}}{L_{f}} \psi_{f} \\ 0 \\ 0 \\ 0 \end{bmatrix}$$

$$(9)$$

where  $T_s = -\frac{L_{md}}{I_s} \psi_f I_{sq} - (L'_d - L_q) I_{sq} I_{sd}$ .

A.2. Induction generator model (squirrel-cage rotor)

$$\dot{\psi}_{rq} = \frac{1}{\tau'_{o}} (-\psi_{rq} + L_{m}I_{aq}) + \omega_{b}(\omega_{s} - \omega_{a})\psi_{rd} 
\dot{\psi}_{rd} = \frac{1}{\tau'_{o}} (-\psi_{rd} + L_{m}I_{ad}) - \omega_{b}(\omega_{s} - \omega_{a})\psi_{rq} 
\begin{bmatrix} R_{a} & -\omega_{s}L'_{s} & 1 & 0 \\ \omega_{s}L'_{s} & R_{a} & 0 & 1 \\ r_{2} & -\omega_{s}L_{2} & (\omega_{s}^{2}C_{a}L_{2} - 1) & \omega_{s}R_{2}C_{a} \\ \omega_{s}L_{2} & R_{2} & -\omega_{s}R_{2}C_{a} & (\omega_{s}^{2}C_{a}L_{2} - 1) \end{bmatrix} \begin{bmatrix} I_{aq} \\ I_{ad} \\ V_{aq} \\ V_{ad} \end{bmatrix}$$

$$+ \begin{bmatrix} 0 & 0 \\ 0 & 0 \\ 1 & 0 \\ 0 & 1 \end{bmatrix} \begin{bmatrix} V_{bq} \\ V_{bd} \end{bmatrix} = \begin{bmatrix} \omega_s \frac{L_m}{L_r} \psi_{rd} \\ -\omega_s \frac{L_m}{L_r} \psi_{rq} \\ 0 \\ 0 \end{bmatrix}. \tag{11}$$

A.3. Wind-turbine drive train model (shaft between rotor turbine and the IG)

$$\dot{\theta}_c = \omega_t - \omega_a 
\dot{\omega}_t = \frac{1}{J_t} \left( \frac{1}{2} C_p \rho A_r \frac{v_w^3}{\omega_t} - C_c \theta_c - (D_t + D_c) \omega_t + D_c \omega_a \right) 
\dot{\omega}_a = \frac{1}{J_a} \left( C_c \theta_c + D_c \omega_t - (D_a + D_c) \omega_a - T_a \right).$$
(12)

A.4. Network model

$$I_{sa} + I_{ia} - I_{la} - I_{ac,a} = 0, I_{sd} + I_{id} - I_{ld} - I_{ac,d} = 0 (13)$$

$$\begin{split} I_{lq} &= \left(\frac{R_3}{R_3^2 + X_3^2} + \frac{1}{r_{dump}}\right) V_{bq} + \frac{X_3}{R_3^2 + X_3^2} V_{bd} \\ I_{ld} &= -\frac{X_3}{R_3^2 + X_3^2} V_{bq} + \left(\frac{R_3}{R_3^2 + X_3^2} + \frac{1}{r_{dump}}\right) V_{bd} \end{split}$$

$$\begin{split} I_{iq} &= I_{aq} + \omega_s C_a V_{ad}, \qquad I_{id} = I_{ad} - \omega_s C_a V_{aq}, \\ I_{ac,q} &= \frac{-\omega_s C_{filt}}{1 - \omega_s^2 C_{filt} L_{filt}} V_{cd} + \frac{1}{1 - \omega_s^2 C_{filt} L_{filt}} I_{cq}, \\ I_{ac,d} &= \frac{\omega_s C_{filt}}{1 - \omega_s^2 C_{filt} L_{filt}} V_{cq} + \frac{1}{1 - \omega_s^2 C_{filt} L_{filt}} I_{cd}. \end{split}$$

#### A.5. Symbols

 $C_a,\,\omega_a$ : capacitor bank and angular speed of wind turbine  $L_{md}$ ,  $L_d^{"}$ : d-axis field mutual inductance and transient induc-

 $I_{lq}$ ,  $I_{ld}$ : current component of the load  $V_{sq}$ ,  $V_{sd}$ : stator terminal voltage components of SG  $E_{fd}$ ,  $\psi_f$ : field voltage and field flux linkage of SG

 $\omega_s$ ,  $\omega_t$ : bus frequency (or angular speed of SG) and IG rotor  $\tau_{do}'$ ,  $\tau_o'$ : transient open circuit time constant  $T_s$ ,  $T_a$ : air gap torque of SG and IG  $J_s$ ,  $D_s$ : inertia and frictional damping of SG

 $\psi_{rq}, \psi_{rd}$ : rotor flux linkage components of SG  $R_s, R_a, L_s', L_r$ : stator and rotor resistance and inductance of SG  $R_1, R_2, L_1, L_2$ : resistance and reactance between SG and IG and bus  $I_{sq}$ ,  $I_{sd}$ ,  $I_{iq}$ ,  $I_{id}$ : current component of SG and IG into the bus

 $I_{sq}$ ,  $I_{sd}$ ,  $I_{iq}$ ,  $I_{id}$ : current component of SG and iG into the bus  $I_{aq}$ ,  $I_{ad}$ ,  $V_{aq}$ ,  $V_{ad}$ : stator terminal current and voltage of IG  $L_q$ ,  $L_d$ ,  $L_f$ ,  $L_m$ : q-, d-axis, field, and mutual inductance of SG  $I_{cq}$ ,  $I_{cd}$ ,  $V_{cq}$ ,  $V_{cd}$ :AC side current and voltage of the converter  $I_{ac,q}$ ,  $I_{ac,d}$ : the AC side current before the filters  $Q_f$ : fuel flow rate into the combustion chamber

 $\vec{Q_d}$ : fuel flow rate at the governor chamber valve

 $p_0$ : zero torque pressure when running idle

 $\tau_d$ : time delay of combustion

 $k_v$ : stroke volume of the engine

 $k_c$ : a constant describing efficiency of combustion

 $\theta_{cl}$ : torsional angle between the engine and the generator shaft

 $\rho$ : air density  $C_p$ : power efficient coefficient

 $A_r$ : swept area of the rotor

 $v_w$ : wind velocity

 $R_3, X_3$ : equivalent load resistance and reactance

#### A.6. Parameter base values

Terms	Symbols	Parameters
Angular	$\omega_b$	$2\pi 50 \text{ rad/s}$
speed/frequency		
Power	$S_b = P_b = Q_b$	55 000 VA
Line AC voltage	$V_b$	230 V (rms)
DC voltage	$V_{dc}$	230 V
AC current	$I_b = S_b / \sqrt{3} V_b$	138 A
DC current	$I_{dc} = S_b/V_{dc}$	239 A
Resistance	$R_{base} = V_b^2 / S_b$	$0.96~\Omega$
Inductance	$L_{base} = R_{base}/\omega_b$	3.06 mH
Capacitance	$C_{base} = 1/(R_{base}\omega_b)$	3.31 mF
Torque	$T_b = S_b/\omega_b$	175.1 N m
Moment of inertia	$J_{base} = S_b/\omega_b^2$	$0.557 \text{ kg m}^2/\text{s}$
Torsional stiffness	$C_{T,base} = T_{base}/\text{rad}$	175.1 N m/rad
Torsional damping	$D_{T,base} = T_{base}/\omega_b$	0.557 N ms/rad

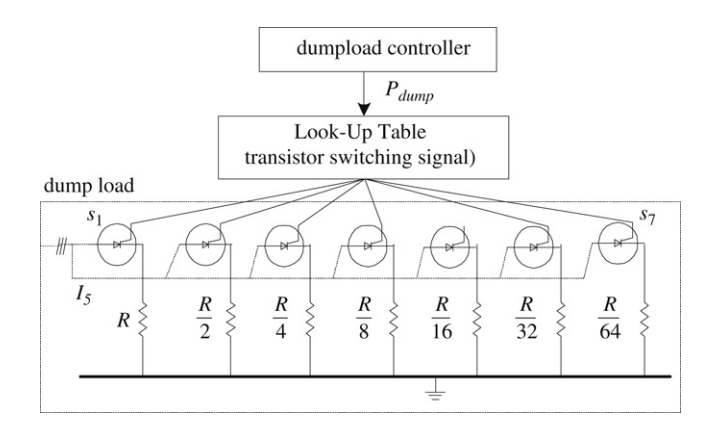


Fig. 10. The structure of the dumpload with binary resistor sizing.

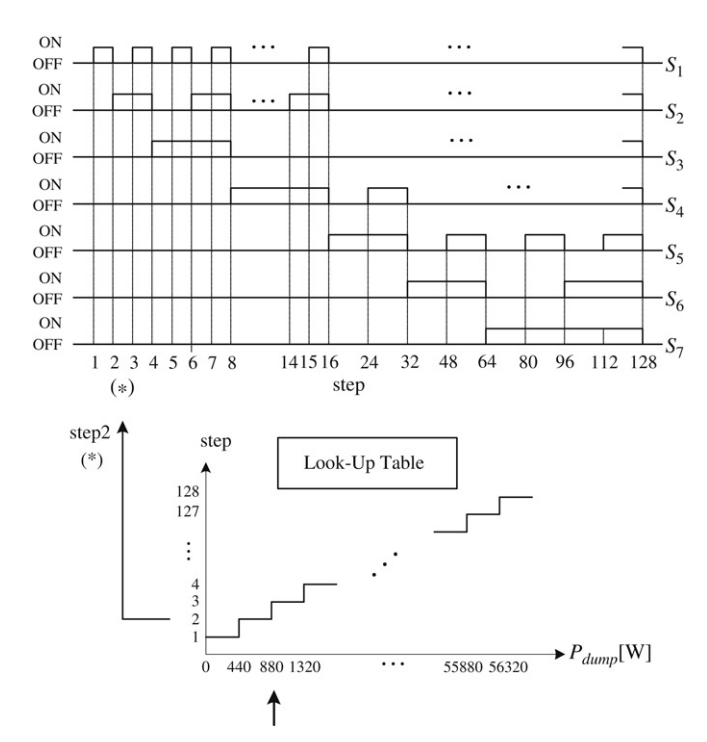


Fig. 11. Transistor switching signal.

#### Appendix B. Dumpload model

Fig. 10 is the three-phase dumpload, where each phase consists of 7 transistor-controlled resistor banks with binary resistor sizing in order to minimize quantum effects and provide more-or-less linear resolution. Fig. 11 shows how the transistors are switched to meet the required power. For example, based on the rated AC line voltage of 230 V and per-phase resistance of  $R (=120 \ \Omega)$ , if the required dumpload power from the dumpload controller is 880 W, Step-2 is identified, and only switch  $S_2$  is turned ON.

#### References

Chedid, R. B., Karaki, S. H., & Chadi, E. C. (2000). Adaptive fuzzy control for winddiesel weak power systems. *IEEE Transactions on Energy Conversion*, 15(1), 71–78.

Feris, L. L. (1990). Wind energy conversion system. New Jersey: Prentice Hall.

Hagan, M. T., & Menhaj, M. B. (1994). Training feedforward networks with the Marquardt algorithm. *IEEE Transactions on Neural Networks*, 5(6), 989–993.

Haley, P., Soloway, D., & Gold, B. (1999). Real-time adaptive control using neural generalized control. In *Proc. American control conference* (pp. 4278-4282).

Haykin, S. (1998). Neural networks: A comprehensive foundation. New Jersey: Prentice Hall.

Harnold, C. -L. -M., Lee, K. Y., Lee, J. -H., & Park, Y. -M. (1998). Free model based adaptive inverse control for dynamic systems. In Proc. the 37th IEEE conference on decision and control (p. 507).

Hunter, R., & Elliot, G. (1994). Wind-diesel systems. New York: Cambridge University.

International Electrotechnical Commission, (1975). Publication 34-10, Rotating electrical machines, Part 10: Conventions for description of synchronous machines. Geneva.

Karaki, S. H., Chedid, R. B., & Ramadan, R. (2000). Probabilistic production costing of diesel-wind energy conversion systems. *IEEE Transactions on Energy Conversion*, 15(3), 284–289.

Kawato, M., Furukawa, K., & Suzuki, R. (1987). A hierarchical neural-network model for control and learning of voluntary movement. *Biological Cybernetics*, 57, 169–185.

Krause, P. C., Wasynczuk, O., & Sudhoff, S. D. (1986). Analysis of electrical machinery. New York: McGraw-Hill.

Madsen, P. P. (1995) Neural network for optimization of existing control systems. In *Proc. IEEE international joint conference on neural networks* (pp. 1496–1501).

Nakanishi, J., & Schaal, S. (2004). Feedback error learning and nonlinear adaptive control. *Neural Networks*, 17, 1453–1465.

Ng, G. W. (1997). Application of Neural Networks to adaptive control of nonlinear systems. John Wiley and Sons Inc.

Pandiaraj, K., Taylor, P., & Jenkins, N. (2001). Distributed load control autonomous renewable energy systems. *IEEE Transactions on Energy Conversion*, 16(1), 14–19

Park, Y. M., Choi, M. S., & Lee, K. Y. (1996). An optimal tracking neuro-controller for nonlinear dynamic systems. *IEEE Transactions on Neural Networks*, 7(5), 1099–1110

Park, Y. M., Moon, U. C., & Lee, K. Y. (1995). A self-organizing fuzzy logic controller for dynamic systems using fuzzy auto-regressive moving average (FARMA) model. *IEEE Transactions on Fuzzy Systems*, 3(1), 75–82.

Park, Y. M., Moon, U. C., & Lee, K. Y. (1996). A self-organizing power system stabilizer using fuzzy auto-regressive moving average (FARMA) model. *IEEE Transactions* on *Energy Conversion*, 11(2), 442–448.

Passino, K. M. (1997). Fuzzy control: Theory and applications. Addison Wesley Publishing.

Tripathy, S. C., Kalantar, M., & Balasubramanian, R. (1991). Dynamics and stability of wind and diesel turbine generator with superconducting magnetic energy storage unit on an isolated power system. *IEEE Transactions on Energy Conversion*, 6(4), 579–585.

Yen, J., & Langari, R. (1999). Fuzzy logic: Intelligence, control, and information. Prentice Hall.



Hee-Sang Ko received his B.S. degree in Electrical Engineering from Cheju National University, Jeju, Korea, in 1996, his M.Sc. degree in Electrical Engineering from Pennsylvania State University, University Park, USA, in 2000, and his Ph.D. in Electrical and Computer Engineering from the University of British Columbia, Vancouver, Canada, in 2006. He is a researcher in the cooperation planning team at Samsung Heavy Industries Company, Korea. His research interests include wind power generation, power system voltage and transient stability, data processing for power system security

analysis, electricity market analysis, and system identification.



Kwnag Y. Lee received his B.S. degree in Electrical Engineering from Seoul National University, Korea, in 1964, M.S. degree in Electrical Engineering from North Dakota State University, Fargo, in 1968, and Ph.D. degree in System Science from Michigan State University, East Lansing, in 1971. He has been with Michigan State, Oregon State, Univ. of Houston, the Pennsylvania State University, and Baylor University where he is currently a Professor and Chair of Electrical and Computer Engineering. His interests include power system control, operation, planning, and intelligent system applications

to power systems. Dr. Lee is a Fellow of IEEE, Associate Editor of IEEE Transactions on Neural Networks, and Editor of IEEE Transactions on Energy Conversion. He is also a registered Professional Engineer.



Min-Jae Kang received the B.S. degree in Electrical Engineering from Seoul National University in 1982 and Ph.D. degree in Electrical & Computer Engineering from University of Louisville in 1991. Since 1992, he has been with the School of Electrical and Electronic Engineering at Cheju National University, where he is currently a professor.



Ho-Chan Kim received the B.S., M.S., and Ph.D. degrees in Control & Instrumentation Engineering from Seoul National University in 1987, 1989, and 1994, respectively. He was a research staff in 1994 and 1995 at the Korea Institute of Science and Technology (KIST). Since 1995, he has been with the Department of Electrical Engineering at Cheju National University, where he is currently a professor. He was a Visiting Scholar at the Pennsylvania State University in 1999. His research interests include wind power control, electricity market analysis, and grounding systems.